Improving Digital-to-analog Converter Linearity by Large High-frequency Dithering

Arnfinn A. Eielsen, *Member, IEEE,* and Andrew J. Fleming, *Member, IEEE*

Abstract

A new method for reducing harmonic distortion due to element mismatch in digital-to-analog converters is described. This is achieved by using a large high-frequency periodic dither. The reduction in non-linearity is due to the smoothing effect this dither has on the non-linearity, which is only dependent on the amplitude distribution function of the dither. Since the high-frequency dither is unwanted on the output on the digital-to-analog converter, the dither is removed by an output filter. The fundamental frequency component of the dither is attenuated by a passive notch filter and the remaining fundamental component and harmonic components are attenuated by the low-pass reconstruction filter. Two methods that further improve performance are also presented. By reproducing the dither on a second channel and subtracting it using a differential amplifier, additional dither attenuation is achieved; and by averaging several channels, the noise-floor of the output is improved. Experimental results demonstrate more than 10 dB improvement in the signal-to-noise-and-distortion ratio.

Index Terms

digital analog conversion, linearization techniques, convolution, nonlinear distortion, dither, element mismatch

EDICS Category: ACS320, ACS210A5, NOLIN100

A. A. Eielsen and A. J. Fleming are with the School of Electrical Engineering and Computer Science, University of Newcastle, Callaghan, NSW 2308, Australia (e-mail: {ae840, andrew.fleming}@newcastle.edu.au).

Improving Digital-to-analog Converter Linearity by Large High-frequency Dithering

I. Introduction

Physical implementations of digital-to-analog converters (DACs) introduce non-linearity due to element mismatch which can become be the limiting factor to the performance [1, 2]. An example of this is shown in Fig. 1, which plots the measured power spectrum of a 16-bit DAC on a National Instruments PCIe-7851R card. The harmonic frequency components are caused by the non-linearity of the DAC which results in a signal-to-noise-and-distortion ratio (SINAD) of 94.2 dBc instead of the theoretically achievable 98.1 dBc[1].

In many applications it is desirable to improve the performance of existing DAC systems, hence there is a demand for methods which can be retrofitted with only minor hardware variations.

A. Existing Methods for Mitigation of Element Mismatch

Known methods for reducing the effect of the non-linearity in DACs due to element mismatch include physical component trimming, physical calibration of output current elements, and dynamic element matching [2]–[6], as well as digital calibration using stored level measurements for Δ-Σ modulators [4,7,8].

Component trimming and physical calibration of output current elements can lead to significant improvements in linearity [6,9]. However, component trimming must be done during manufacturing [6], and existing current element calibration techniques require additional circuitry to be included as part of the DAC layout [6,9]. Hence, these methods can not be retrofitted to an existing DAC.

Dynamic element matching (DEM) relies on redundancy in the output elements [2,3], and can be very effective at reducing the effects of element mismatch. A recent implementation of DEM in the form of data-weighed averaging (DWA) was reported in [8] to yield a SINAD improvement of up to 11.4 dB for a 14-bit DAC. If two or more DAC channels are available, element redundancy can in principle be introduced and DEM can be retrofitted to an existing system by summing the channels. When applying this method to an existing system, the main drawbacks are the need for several channels, and increased computational requirements due to the element switching logic. The amount of glitch energy produced by the DACs will likely influence the achievable performance [10].

Similarly, Δ-Σ modulation can be retrofitted to an existing DAC by preprocessing the input signal. However, to obtain good performance, digital calibration [7] or additional DEM is required [4]. The main drawback to using digital calibration is the requirement to measure and store the output levels of the DAC. For a DAC with a large word-size, this is time-consuming and it requires a precision multimeter or a precision analog-to-digital converter (ADC). The levels will also drift with time, due to temperature sensitivity and aging, which necessitates re-measuring of the levels to maintain performance. Computational requirements are also increased due to the noise-shaping filter, storage of the measured levels, and possibly for implementing DEM. Digital calibration was reported in [8] to yield a SINAD improvement of up to 18.0 dB for a 14-bit DAC.

It should also be mentioned that there exist more specialized methods for generating low-distortion sinusoidal signals. These methods include distortion shaping [11,12] and harmonic cancellation [13]–[15].

B. Outline of Proposed Method

The method presented here can also be retrofitted to an existing DAC. Compared to DEM and Δ-Σ modulation, the computational complexity is limited to periodic signal generation. In contrast to Δ-Σ modulation with digital calibration, the method can improve the DAC performance without any knowledge of the non-linearity, which is similar to DEM. Similar to Δ-Σ it requires sufficiently high bandwidth to allow for oversampling. Considering for example control of high-speed flexure-guided nanopositioning devices, the majority of available devices have a bandwidth between 100 Hz to 10 kHz [16], hence many modern high-resolution DACs will have the required bandwidth to allow for oversampling.

The method is based on the fact that a static non-linear function $n(\cdot)$ can, by the application of a suitable periodic dither, be approximated by a smoothed non-linear function $N(\cdot)$ where $\|N\|_\infty \leq \|n\|_\infty$; hence reducing the effects caused by the non-linearity $n(\cdot)$ [17]–[20]. The smoothed non-linearity $N(\cdot)$ is determined by the non-linearity $n(\cdot)$ and the

[1]A higher SINAD can be achieved with oversampling. One hundred times oversampling, OSR $= 100$, has been used in Fig. 1; hence the theoretical SINAD should be improved by another $10\log_{10}(\text{OSR}) = 20$ dB.

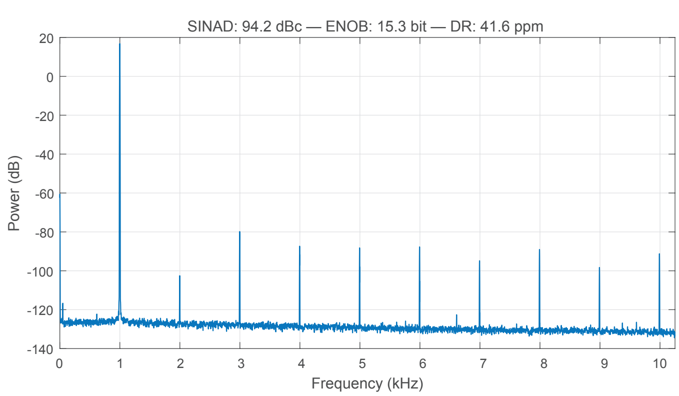

Fig. 1. Power spectrum from a 16-bit DAC with element mismatch.

amplitude distribution function of the dither. The validity of the approximation is mainly dependent on the frequency of the dither, hence it is termed high-frequency (HF) dither.

The HF dither will reduce the effect of the non-linearity below the dither frequency. Similar to Δ-Σ modulation, there is a large amount of undesired high-frequency power in the output signal which must be removed. Contrary to Δ-Σ modulation, most of the undesired output signal content is periodic and independent of the input signal. A significant amount of this can be removed by notch filters and the low-pass reconstruction filter.

By reproducing the HF dither on a secondary DAC and subtracting the signal using a differential amplifier, additional reduction of the unwanted signal content can be achieved. The increased noise-floor due to the reduced effective range can be improved by averaging over several channels.

C. Dithering Uniform Quantizers

Dither is a well-researched topic for mitigation of quantization effects in data-converters [21]–[26]. The non-linearity introduced due to uniform quantization will, similar to element mismatch, introduce harmonic distortion. Contrary to element mismatch, by using a suitable dither, it is possible to completely remove harmonic distortion due to uniform quantization [21,25]. When dithering a uniform quantizer, the main goal for dithering is to decorrelate the quantization error from the input signal and to increase the effective resolution of the data-converter. Many types of dither have been investigated, including sinusoidal or periodic dithers [27]–[30], and stochastic dithers [29]–[32].

D. Dithering Quantizers With Element Mismatch

Dither will also affect non-linearity in the form of element mismatch. This is the main focus of this article. The effects and improvements due to dither in data-converters with element mismatch have previously been studied, but this is limited to stochastic dithers [33]–[38]. For ADCs, the stochastic dither used can be large in amplitude, but averaging is subsequently used to reduce the impact and achieve improved effective resolution. For DACs, the dither is either small in amplitude (on the order of a few least significant bits), or it is bandwidth limited such that the power is outside the desired baseband. A SINAD improvement of 4 dB for a 9-bit DAC utilizing the latter technique was reported in [38].

It is known that in closed-loop control systems with static non-linearities, sinusoidal or periodic dithers can improve the performance [17]–[20]. Here, the theory of periodic dithering in closed-loop control systems with static non-linearities is applied to digital-to-analog conversion. The static non-linearity in DACs is due to element mismatch.

E. Applications

The main intended application of the method is to improve the performance in control systems for nanopositioning and metrology [16,39,40]. For such applications, the reduction of unknown non-linearities also reduces systematic measurement errors that can not be reduced by averaging, as would be the case for stochastic errors [39]. Hence, an improvement in SINAD is beneficial, even if the signal-to-noise ratio (SNR) is reduced. However, many digital signal processing platforms used for control are often equipped with several DAC channels. Thus, a reduced SNR due to a large HF dither can therefore be recovered using channel averaging if unused DACs are available.

By application of the presented method, it should be possible to improve the linearity of lower-end DACs, and recover the noise-floor by using several DACs. This can potentially be a cost effective solution to obtain comparable performance to a single high-end DAC.

II. Contributions

Three different methods are presented. The main contribution is the application of a large high-frequency (HF) periodic dither with uniform amplitude distribution in order to reduce the effect of the static non-linearity due to element mismatch in a DAC, and the subsequent removal of the HF dither in the output by using an analog notch and low-pass filter.

Next, the limited attenuation performance of the notch and low-pass filter with regards to the HF dither is counteracted by reproducing the HF dither on a secondary DAC and subtracting the signal using a differential amplifier.

Lastly, due to the large amplitude of the HF dither the effective range of the DAC is reduced. The subsequent increase of the noise-floor can be improved by averaging several channels. Channel averaging will not mitigate element mismatch, but it will reduce the stochastic component in the output signal.

III. Noise and Distortion in DACs

There are several non-ideal effects and artefacts that occur in a DAC. The fundamental sources are aliasing and quantization. These effects are due to the fact that a DAC operates on a signal that is discretized both in time and value [23]. Aliasing occurs because sampling a signal in time will generate repeated spectra over the Nyquist-frequency (half the sampling rate) [41,42]. Quantization is the process of mapping a large set of values to a smaller set of values, therefore it discards some values and introduces a signal dependent error [43,44].

The main secondary effects include non-linearity due to element mismatch, and thermal and semiconductor noise generated by the components in the DAC. Element mismatch causes the actual output levels of the DAC to deviate from the ideal levels. This generates both a static error as well as harmonic and intermodulation distortion [6]. It is also the main limitation to the effectiveness of Δ-Σ modulation [2]. The main sources of thermal and semiconductor noise are the resistor network producing the output voltage levels, the voltage reference, and the output buffer [6,45,46].

A. Harmonic Distortion

A static non-linearity $n(w)$ will generate harmonic distortion if it is excited by a sinusoidal signal. Harmonic distortion is the presence of signal components at multiples of the frequency ω_0 in the output of the function $n(w)$. Element

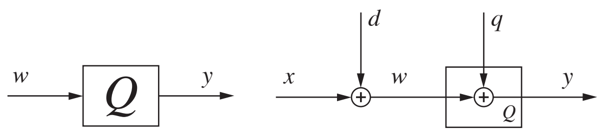

(a) Quantizer. (b) Dithered quantizer.

Fig. 2. Uniform quantizer model.

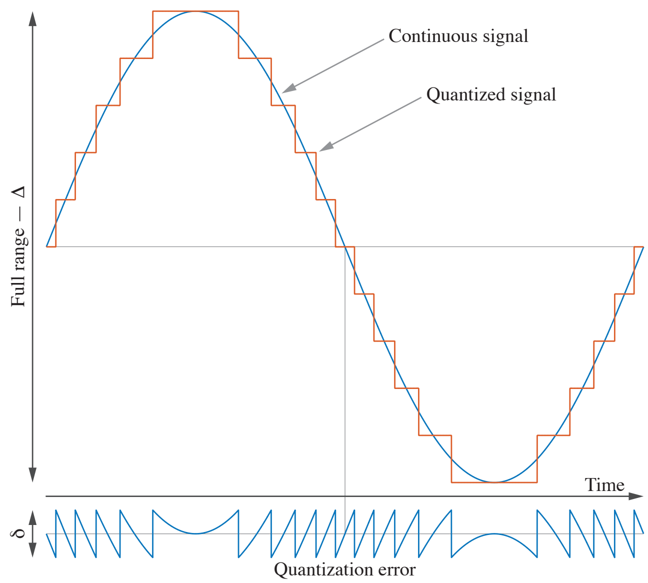

Fig. 3. Sinusoidal waveform quantized by a mid-tread uniform quantizer.

mismatch can be well approximated by a polynomial; a Taylor series. The number of higher order harmonic components is related to the order of the polynomial [6,47]–[49].

B. Intermodulation Distortion

If the non-linearity $n(w)$ is excited by multiple sinusoidal signals with distinct frequencies, there will be intermodulation components in addition to the harmonic components. The intermodulation components appear at sums and differences of multiples of the input frequencies, and can therefore appear below the frequency of the input signal with the lowest frequency. Increasing the order of the polynomial describing the non-linearity or the number of frequency components in the input will generate a higher number of harmonic components and intermodulation components [6,47,48,50,51].

C. Uniform Quantization

A quantizer is represented by the block-diagram symbol in Fig. 2(a). A quantizer is an operator that takes the input values w from a large set and maps them to discrete values y in a smaller set. A uniform quantizer maps to equidistant values with a step-size δ, called the quantization step-size or the least significant bit (LSB). The quantizer is a discontinuous non-linear function that will generate harmonic and intermodulation distortion [52,53].

A DAC typically has 2^B number of levels, where B is the word-size (bits). The quantization step-size is

$$\delta = \frac{\Delta}{(2^B - 1)} \tag{1}$$

where Δ is the output range of the DAC. A mid-tread uniform quantizer is defined using the truncation operator $T(w)$

$$k = T(w) = \left\lfloor \frac{w}{\delta} + \frac{1}{2} \right\rfloor \tag{2}$$

where $\lfloor \cdot \rfloor$ denotes the floor operator. The truncation operator is a discontinuous function. The output y of the quantizer given an input w is

$$y = Q(w) = \delta T(w) = \delta k\,. \tag{3}$$

A mid-tread quantizer is illustrated in Fig. 3 and the term means that zero will be part of the set of output values.

1) Dithering the Uniform Quantizer: For frequency-rich input signals and when using quantizers with $B = 7$ bits or more, the quantization error

$$q(w) \triangleq y - w = Q(w) - w\,. \tag{4}$$

is often modeled as an additive, zero-mean, and uniformly distributed white-noise signal with variance

$${\sigma_q}^2 = \frac{\delta^2}{12}\,. \tag{5}$$

This is called Bennett's classical model of quantization, or the pseudo quantization noise (PQN) model [6,23,25,52].

If the input signal is narrow-band and/or small relative to the quantization step-size, for example if it is a small-amplitude sinusoidal signal, the model is no longer valid, thus introducing undesirable spuriae [25,31,43]. This is often the case in technical applications, where signals such as steps, sinusoids, and triangle-waves are common. The PQN model can be made valid by the addition of a dither d, as indicated in Fig. 2(b).

If the dither is subtracted from the output, perfect decorrelation of quantization noise from the input signal is possible [21]. However, due to the difficulty of perfectly reproducing and subtracting a small noise dither, the effect of using subtractive dithering is reduced in practice [25].

The total output error

$$\varepsilon \triangleq y - x\,, \tag{6}$$

with non-subtractive dithering becomes, using (4),

$$\varepsilon = Q(x + d) - x = d + q(x + d)\,. \tag{7}$$

The signal ε can be made stationary [54] with a constant first and second moment that is independent of the signal x, by using a dither d with a triangular probability distribution function (TPDF) of range $[-\delta, \delta]$ [25,26],

$$\frac{1}{\delta}\,\text{triang}\left(\frac{v}{\delta}\right) = \begin{cases} \frac{1}{\delta}\left(1 - \frac{|v|}{\delta}\right) & |v| \leq \delta \\ 0 & |v| > \delta \end{cases}\,. \tag{8}$$

A dither signal with a TPDF can be generated by exciting the high-pass filter

$$H(z^{-1}) = 1 - z^{-1} \tag{9}$$

by uniformly distributed white noise in the interval $[-\delta/2, \delta/2]$ [25]. The summation or difference of two samples from a sequence of independent and identically distributed

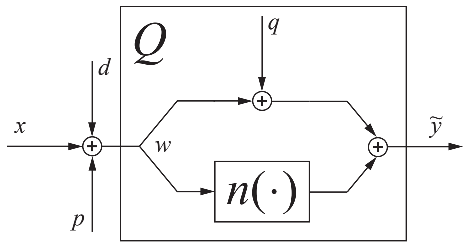

Fig. 4. Non-linear quantizer model.

(IID) samples drawn from a uniform distribution means that the output distribution will be the convolution of two uniform distributions [55]; hence the output will have a TPDF. The power spectral density (PSD) function of the signal is

$$S_d(f) = \frac{\delta^2}{6f_s}\left(1 - \cos\left(\frac{2\pi}{f_s}f\right)\right) \tag{10}$$

where f_s is the sampling frequency for the filter $H(z^{-1})$.

Non-subtractive dithering using a noise signal with TPDF in the interval $[-\delta, \delta]$ eliminates the distortion due to uniform quantization and allows the total output error to be considered a stationary white-noise signal. However, the variance of the total output error ε is three times larger,

$${\sigma_\varepsilon}^2 = {\sigma_d}^2 + {\sigma_q}^2 = \frac{\delta^2}{4}\ , \tag{11}$$

but the high-pass frequency distribution means that a large portion of the dither noise can be attenuated by the low-pass reconstruction filter.

IV. Non-linear Quantizer

All digital-to-analog converters have *element mismatch*. This means that the actual levels deviate from the ideal equidistant levels (3). The element mismatch is typically modelled as an additive static non-linearity. Hence, the output of the quantizer in (3) is modified to be

$$\tilde{y}(k) = y(k) + \delta\mathrm{INL}(k) = \delta k + \delta\mathrm{INL}(k)\ . \tag{12}$$

The static non-linear function $\mathrm{INL}(k)$ is called the integral non-linearity and the standard definition is [6]

$$\mathrm{INL}(k) \triangleq \frac{\tilde{y}(k) - \delta k}{\delta}\ . \tag{13}$$

The effect of the non-linearity due to the input w seen on the output is taken to be described by the function $n(w)$:

$$n(w) = \delta\mathrm{INL}\,(k)|_{k=T(w)} \tag{14}$$

This is a discontinuous function due to the truncation operator. The model of the non-linear quantizer is shown in Fig. 4.

A. Smoothing Due to High-frequency Dither

If the non-linear function $n(w)$ is excited by the sum $w = x + p$ of an arbitrary signal x and a periodic dither p with sufficiently high frequency and amplitude, the function $n(x+p)$ can be approximated by another function $N(x)$ with a narrower non-linear sector, $\|N\|_\infty \leq \|n\|_\infty$. Hence, the effects caused by the non-linearity are reduced [17]–[20].

The definition of the smoothed non-linearity $N(x)$ is:

$$N(x) \triangleq \int_{\mathbb{R}} n(x+v)\mathrm{d}F_p(v) \tag{15}$$

Here $F_p(v)$ is the amplitude distribution function of the high-frequency (HF) dither p. The method relies on the equivalence of the above Lebesgue-Stieltjes integral and the time-average over one period τ of the periodic dither, where x is assumed to be constant for the duration of the period [20]:

$$\int_{\mathbb{R}} n(x+v)\mathrm{d}F_p(v) = \frac{1}{\tau}\int_0^\tau n\left(x + p(t)\right)\mathrm{d}t \tag{16}$$

The error introduced by the assumption of x being piecewise constant with duration τ goes to zero as $\tau \to 0$. The error is quantified in Sec. IV-B. If the distribution F_p is absolutely continuous, the averaging effect of the dither p on the non-linearity $n(w)$ can be found by evaluation of the Lebesgue-Stieltjes integral of the form:

$$\int_{\mathbb{R}} n(x+v)\mathrm{d}F_p(v) = \int_{\mathbb{R}} n(x+v)f_p(v)\mathrm{d}v \tag{17}$$

Here, $f_p(v)$ is the amplitude density function, defined as:

$$f_p(v) \triangleq \frac{\mathrm{d}}{\mathrm{d}v}F_p(v) \tag{18}$$

The smoothed non-linearity $N(x)$ can be found as the cross-correlation of the function $n(w)$ and the amplitude density function of the dither. A signal with uniform amplitude density

$$f_p(v) = \frac{1}{2A}\mathrm{rect}\left(\frac{v}{2A}\right) = \begin{cases} \frac{1}{2A} & |v| \leq A \\ 0 & |v| > A \end{cases} \tag{19}$$

is an example of a signal with an absolutely continuous amplitude distribution function. One realization of such a signal is the triangle wave, which is the dither used in the experiments. If $f_p(v)$ is even, (17) can be found as a convolution product, and by using the triangle wave dither this is equivalent to filtering $\mathrm{INL}(k)$ by a filter with Fourier transform

$$\int_{-\infty}^{\infty} \delta f_p(v)\mathrm{e}^{-j2\pi\xi v}\mathrm{d}\xi = \delta\mathrm{sinc}(2A\xi)\ , \tag{20}$$

which has a low-pass characteristic. Hence, the dither attenuates the variations in the INL. Increasing the dither amplitude A increases the smoothing of the INL.

Even though the dither will reduce the harmonic distortion of the arbitrary carrier x, there will still be intermodulation between the dither p and the carrier x. The intermodulation depends on the original non-smoothed INL. However, this might not be a problem in many practical situations, as the dither frequency should be high in order for (16) to hold.

B. Approximation Error

Given a signal $x : [0, \tau] \mapsto \mathbb{R}$ with a Lipschitz constant L_x. This signal can be approximated by a constant $\tilde{x}$ in each interval τ, which is the period of the dither. Hence, $\tilde{x}$ satisfies

$$\min_{t\in[0,\tau]} x(t) \leq \tilde{x} \leq \max_{t\in[0,\tau]} x(t) \tag{21}$$

If F_p is absolutely continuous with a bounded derivative $L_F = \sup_{v\in\mathbb{R}} |f_p(v)| < \infty$, then [20]:

$$\left|\int_0^\tau n\left(x(t)+p(t)\right)\mathrm{d}t - \int_0^\tau n\left(\tilde{x}+p(t)\right)\mathrm{d}t\right| \le 2L_F L_x \left\|n\right\|_{TV} \tau^2 \quad (22)$$

The expression $\|\cdot\|_{TV}$ denotes the total variation. If $n : \mathbb{R} \mapsto \mathbb{R}$ is a function, the total variation $\|n\|_{TV}$ is defined to be the supremum [56,57]

$$\|n\|_{TV} \triangleq \sup_{w_0\le\ldots\le w_M} \sum_{i=1}^{M} |n(w_i) - n(w_{i-1})| \quad (23)$$

where the supremum ranges over all finite increasing sequences $w_0, \ldots, w_k$ of real numbers with $M \ge 0$. If $\|n\|_{TV}$ is finite, $n(w)$ has bounded variation. Hence, the function $n(w)$ can be discontinuous, but it must be bounded.

The expression (22) means that the approximation error is most sensitive to the dither period τ; and if $\tau \to 0$, the error goes to zero. If a uniform dither is applied to a DAC with a non-linearity described by $\text{INL}(k)$, the Lipschitz constant is $L_F = 1/A$ for the uniform distribution, $L_x = \gamma\omega_0$ for a sinusoidal input signal $\gamma_0 \sin(\omega_0 t)$, and the total variation $\|n\|_{TV}$ can be found from

$$\|n\|_{TV} = \delta \sum_k |\text{DNL}(k)| \quad (24)$$

where

$$\text{DNL}(k) = \text{INL}(k) - \text{INL}(k-1) \;, \quad (25)$$

which is called the differential non-linearity [6].

C. Summary of the High-frequency Dither Method

By adding a periodic high-frequency (HF) dither with sufficient amplitude, such as a triangle-wave, to the carrier signal sent to a DAC, the distortion due to element mismatch can be reduced. Element mismatch is expressed using the integral non-linearity (INL) (13). The dither amplitude A determines the amount of smoothing of the INL. The attenuation of variations in the INL with respect to the input voltage by the equivalent ideal low-pass filter in (20) will increase as A increases. That is, the main lobe of the function $\delta\text{sinc}(2A\xi)$ becomes narrower as A increases.

The validity of the smoothing effect is mainly dependent on the period of the HF dither. The approximation error associated with the cross-correlation product in (17) is expressed in (22), where it can be seen that the choice of dither period will have a larger influence on the approximation error that the amplitude distribution function due to the square-law dependence. A high dither frequency will also ensure that intermodulation products do not appear in the baseband.

V. Averaging Using Several Channels

With regards to uniform quantization, since a stochastic dither d with a TPDF in the range $[-\delta, \delta]$ makes the first and second moment of the total output error ε independent of the input signal and spectrally white, it should be possible to reduce the noise-floor by averaging over several channels, if each channel is dithered using independent dithers. However, averaging will have negligible impact on element mismatch.

Considering the non-linear output $\tilde{y} = Q(w) + n(w)$, the output without HF dither is

$$\tilde{y}_i = x + d_i + q_i + n_i(x + d_i) \quad (26)$$

and the total error with non-linear output for one channel i is

$$\tilde{\varepsilon}_i = \tilde{y}_i - x = \varepsilon_i + n_i(x + d_i) \approx \varepsilon_i + n_i(x) \;. \quad (27)$$

Similarly the output with HF dither p is

$$\tilde{y}_i = x + p + d_i + q_i + n_i(x + p + d_i) \quad (28)$$

and the total error with non-linear output and HF dither for one channel i is

$$\tilde{\varepsilon}_i^{\mathrm{p}} = \tilde{y}_i - (x + p) = \varepsilon_i + N_i(x + d_i) \approx \varepsilon_i + N_i(x) \;. \quad (29)$$

By making the assumption that $\sigma_x \gg \sigma_{d_i}$, thus $n_i(x + d_i) \approx n_i(x)$ and $N_i(x + d_i) \approx N_i(x)$, the signals $\{\varepsilon_i\}$ can be considered stationary and stochastic, and $\{n_i(x)\}$ and $\{N_i(x)\}$ can be considered quasi-stationary deterministic signals [54] if $x(t)$ is a quasi-stationary deterministic signal.

The average error for K channels in the two cases are:

$$\bar{e} = \frac{1}{K}\sum_{i=1}^{K} \varepsilon_i + \frac{1}{K}\sum_{i=1}^{K} m_i(x) = \bar{\varepsilon} + \bar{m} \quad (30)$$

where $m_i = n_i$ in the case without dither and $m_i = N_i$ in the case with dither.

Since $\mathrm{E}\left[{\varepsilon_i}^2\right] = {\sigma_\varepsilon}^2$, the variance of the error due to the dithered uniform quantizers can be reduced by a factor of $1/K$:

$$\text{Var}\left(\bar{\varepsilon}^2\right) = \frac{1}{K}{\sigma_\varepsilon}^2 \quad (31)$$

The variance of $\bar{m}$ on the other hand is a sum of correlated signals, therefore the variance is:

$$\text{Var}\left(\frac{1}{K}\sum_{i=1}^{K} m_i\right) = \frac{1}{K^2}\sum_{i=1}^{n}\text{Var}\left(m_i\right) + \frac{2}{K^2}\sum_{i<j}\text{Cov}\left(m_i, m_j\right) \quad (32)$$

DACs often exhibit characteristic non-linearity depending on the topology and production process [6], hence using channels with the same type of DAC, the non-linearity will be very similar among the channels, i.e. $m_i \approx m_j$. The measured INL for all DAC channels used in the experiments is shown in Fig. 5, and confirms this notion for the experimental system. This leads to a high correlation between the channels for the non-linear response. In the special case when $m_i = m_j$ the variance becomes

$$\frac{K}{K^2}\text{Var}\left(m_i\right) + \frac{K(K-1)}{K^2}\text{Var}\left(m_i\right) = \text{Var}\left(m_i\right) \;; \quad (33)$$

hence there would be *no reduction* of the non-linear response due to averaging several channels.

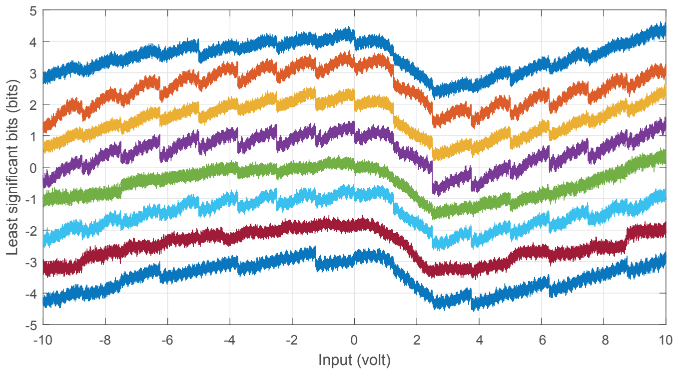

Fig. 5. Measured and de-trended INL for all DAC channels used in the experiments, offset by 1 bit for legibility.

VI. Subtracting the HF Dither

Consider two channels, where one channel produces the carrier signal and the HF dither

$$\tilde{y}_1 = x + p + \varepsilon_1 + m_1,\ m_1 = n_1(x + p + d_1) \tag{34}$$

and the other channel produces only the HF dither

$$\tilde{y}_2 = p + \varepsilon_2 + m_2,\ m_2 = n_2(p + d_1)\ , \tag{35}$$

then the output of a differential amplifier y_d fed with the two signals will be

$$y_d(s) = W_+(s)\,(x(s) + p(s) + \varepsilon_1(s) + m_1(s)) \\ - W_-(s)\,(p(s) + \varepsilon_2(s) + m_2(s))\ \ , \tag{36}$$

where the filters $W_+(s)$ and $W_-(s)$ account for impedance of the non-iverting and inverting input of the amplifier.

If $W_+(s) \approx W_-(s)$, the output is

$$y_d(s) \approx W_+(s)\,(x(s) + \varepsilon_1(s) - \varepsilon_2(s) + m_1(s) - m_2(s))\ . \tag{37}$$

Hence, with closely matched impedances, it is possible to remove the HF dither p in the output, but the variance of the noise component will be twice as large

$$\mathrm{Var}\,(\varepsilon_1 - \varepsilon_2) = 2{\sigma_\varepsilon}^2\ , \tag{38}$$

and the distortion due to the non-linear components m_1 and m_2 is still present. However, if the dither p is large, the removal of this signal will still improve the overall performance.

VII. Numerical and Simulation Results

The voltage levels for all of the eight DAC channels on a National Instruments PCIe-7851R system were measured using an Agilent 34461A precision multimeter and the INL for each channel was computed using these measurements. The de-trended[2] results are shown in Fig. 5.

Using the INL for one of the channels, the smoothed INL using a uniformly distributed dither with an amplitude of 5 V (50%) was computed using the cross-correlation product in (17). The result is shown in Fig. 6. By treating the quantizer

[2]This is done using the `detrend` function in MATLAB, which removes the least-squares straight-line fit from a dataset.

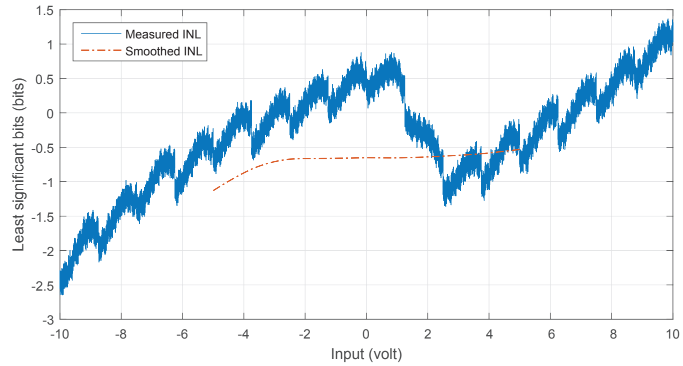

Fig. 6. The measured INL for one of the DAC channels, also shown in Fig. 5, on the NI PCIe-7851R and the result from smoothing the INL with a uniform dither with a range of 50% of the full range (5 volt).

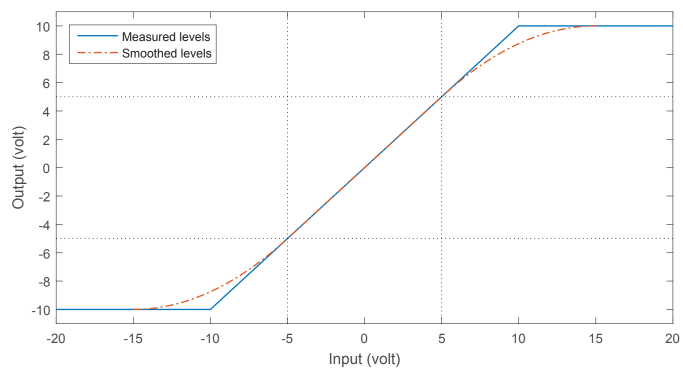

Fig. 7. Treating the quantizer as a saturation non-linearity and increasing the input range, this figure shows the result from smoothing with a uniform dither with a range of 50% of the original range (5 volt).

as a saturation non-linearity and increasing the input range, the smoothed equivalent non-linearity was similarly computed. The result is shown in Fig. 7, which indicates that using a carrier with more than 50% of the range will result in harmonic distortion due to the parabolic interpolation when $|x| > 5$.

The effect of the dither was simulated using the measured INL for one of the channels. An input carrier signal with a 5-V amplitude at 999 Hz *without* the HF dither was applied to both the measured INL and the smoothed INL. The measured INL and the smoothed INL used is shown in Fig. 6. Next, the same carrier combined with a 5-V 50-kHz dither was applied to the measured INL. The three cases are shown in Fig. 8.

Inspecting Fig. 8(a), a reduction in the harmonic distortion can be seen. There is also a good correspondence between the result using the smoothed INL without HF dither and the result using the measured INL with HF dither, confirming that the INL is indeed smoothed by the HF dither and that the approximation error due to a non-zero period for the HF dither is small. In Fig. 8(b) the presence of the HF dither and the intermodulation products between the carrier and the HF dither frequency components can be seen, confirming that most of the unwanted signal content is above the chosen baseband bandwidth of 10 kHz. The input signals used in the simulations are shown in Fig. 9.

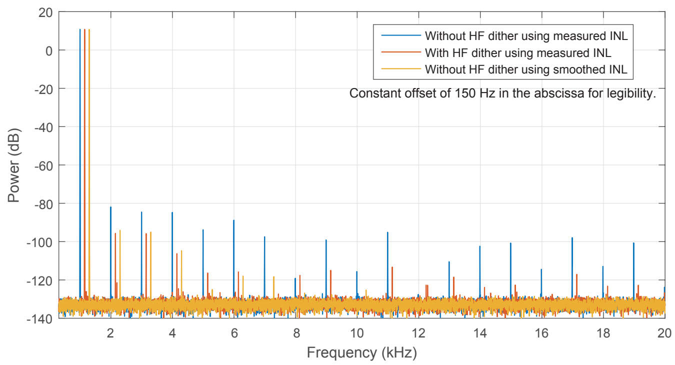

(a) Spectrum up to 20 kHz.

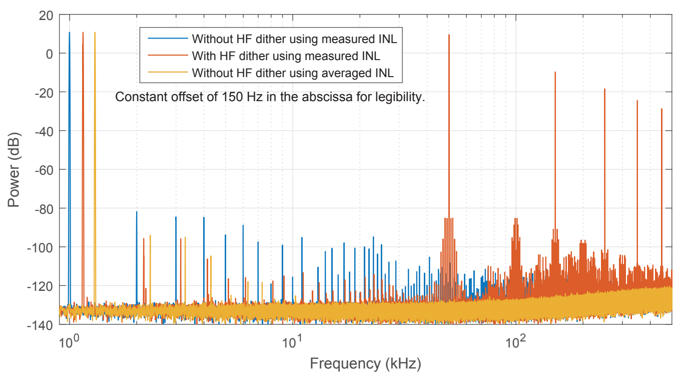

(b) Spectrum up to 500 kHz (Nyquist-rate).

Fig. 8. Simulated spectra showing the effect of the high-frequency (HF) dither.

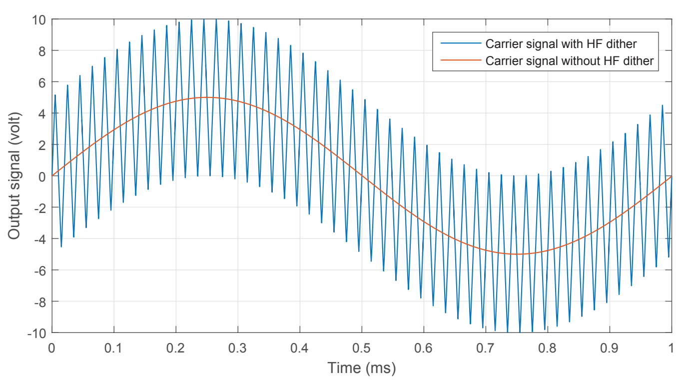

Fig. 9. Time-series showing the carrier and carrier with HF dither which is input to the DAC.

VIII. Experimental Set-up

The experimental set-up is shown in Fig. 10. A National Instruments PCIe-7851R system was used to provide eight 16-bit DAC channels with a sampling rate of up to 1 MS/s. The DAC channels are controlled via the onboard field-programmable gate array (FPGA), and it is possible to stream eight 1-MHz 16-bit wide signals using direct memory access (DMA) from a computer (CPU) running the National Instruments LabView software, which was used to generate the carrier x, high-pass noise dither with TPDF d, and the triangle-wave HF dither p. The experiments were conducted using four different configurations of the set-up in Fig. 10:

1) Using a single channel, $K = 1$, for the carrier and HF dither with the inverting input of the differential amplifier grounded.
2) Using a single channel, $K = 1$, for the carrier and HF dither, and single channel for the HF dither with the inverting input of the differential amplifier connected.
3) Using four channels, $K = 4$, for the carrier and HF dither with the inverting input of the differential amplifier grounded.
4) Using four channels, $K = 4$, for the carrier and HF dither, and four channels for the HF dither with the inverting input of the differential amplifier connected.

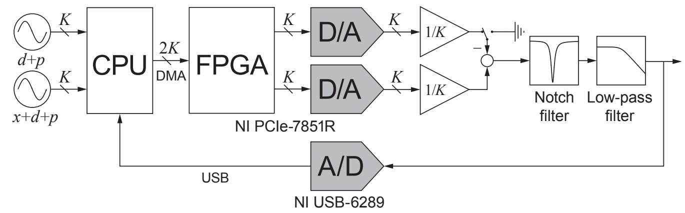

Fig. 10. Experimental set-up.

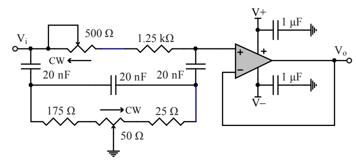

(a) Twin-T notch filter.

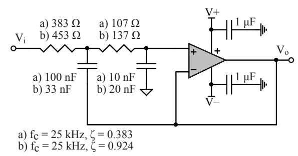

(b) Sallen-Key low-pass filter.

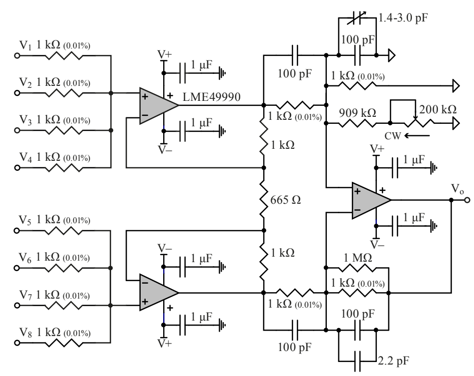

(c) Differential amplifier.

Fig. 11. Analog signal post-processing to remove the HF dither.

In every case the output of the differential amplifier was filtered by the notch and low-pass filter.

The output spectra were measured using a National Instruments USB-6289. It contains an Analog Devices AD7674 18-bit successive approximation analog-to-digital converter (ADC). This ADC has good linear performance, with a spurious-free dynamic range (SFDR) of 120 dBFS for the carrier frequencies considered here. A sampling rate of 625 kS/s was used. The power spectra were generated using power spectrum estimation in LabView, using a frequency resolution of 1 Hz, at least 100 averages, and a Kaiser window [58] with window parameter $\alpha = 38$.

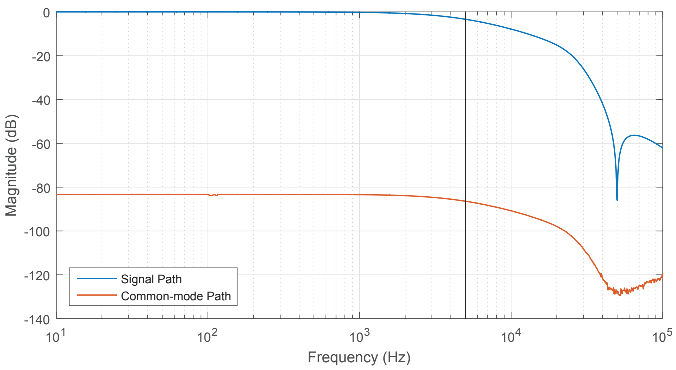

Fig. 12. The magnitude response for signal path through the notch and low-pass filter, as well as the common-mode input path.

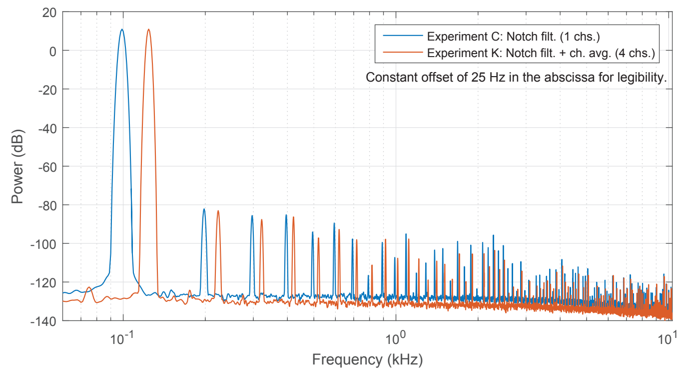

Fig. 13. **Channel averaging:** *Using filter configs. 1) and 3).* Spectra with a 99 Hz carrier signal that show the effect of channel averaging (reduced noise-floor, little effect on harmonic distortion).

A. Differential Amplifier and Notch Filter

The high-frequency power in Fig. 8(b) is unwanted in the output and suitable filtering in required to attenuate it. In the experimental set-up this is achieved with a buffered passive twin-T notch filter and Sallen-Key low-pass (reconstruction) filter, as well as a differential amplifier which is used to subtract the HF dither produced on a secondary channel.

There are several filter topologies that can implement a notch filter, but all-pole topologies are excluded as the notch requires the introduction of a zero. Some of the simplest active topologies suitable for a notch filter in terms of component count and tuning are the Bainter-notch [59] and the gyrator [60]. However, the passive twin-T notch [46,61] in Fig. 11(a) provided the best attenuation, linearity, and noise performance. The notch was tuned to a center-frequency of 50 kHz. The low-pass filter was implemented using the unity-gain Sallen-Key topology [46,62]. To achieve the best noise and linearity performance, high-voltage polypropylene capacitors and low-value resistors were required. To avoid noise peaking, it was also necessary to limit the ratio of capacitors to less than three. This limits the achievable Q-factor; therefore, the Butterworth prototype was utilized since this does not require poles with high Q-factor. The cut-off frequency was $f_c = 25$ kHz. The magnitude response for the combined notch and low-pass filter is plotted in Fig. 12.

A suitable differential amplifier topology is the instrumentation amplifier [46]. Care must be taken to match input impedances in order to obtain matching gain for the inverting and non-inverting input terminals. The gain matching is frequency dependent and mainly depends on the bandwidth of the operational amplifier used. The measured magnitude response for the common-mode path is plotted in Fig. 12, showing an attenuation of the signal difference by more than 80 dB.

IX. Experimental Results

A set of experiments were conducted in order to assess the performance improvement that can be achieved using the HF dither, as well as channel averaging and HF dither subtraction. The measured performance results are summarized in Tab. I, and a comparison of performance metrics for some of the experiments using a 99 Hz carrier is shown in Tab. II. The results are summarized using the following standard metrics [6]: The signal-to-noise ratio,

$$\mathrm{SNR} = 20\log_{10}\left(\sigma_s/\sigma_n\right) \ ,$$

where σ_s is the standard deviation of the carrier signal, and σ_n is the the standard deviation of the noise excluding the harmonic components of the carrier signal. The total-harmonic-distortion,

$$\mathrm{THD} = 20\log_{10}\left(\sigma_d/\sigma_s\right) \ ,$$

where σ_d is the standard deviation of the harmonic components of the carrier signal, excluding any other component. When computing the THD, all the harmonic components up to 10 kHz were used. The signal-to-noise-and-distortion ratio,

$$\mathrm{SINAD} = 20\log_{10}\left(\sigma_s/\sigma_t\right) \ ,$$

where the standard deviation $\sigma_t = \sigma_d + \sigma_n$ accounts for all unwanted components in the output signal. The effective-number-of-bits is defined as

$$\mathrm{ENOB} = (\mathrm{SINAD} - 1.76)/6.02 \ .$$

The ENOB specifies the equivalent resolution of an ideal DAC (with uniform quantization and a uniformly distributed quantization noise with variance ${\sigma_q}^2 = \delta^2/12$). Lastly, the dynamic range is found as

$$\mathrm{DR} = 3/\sqrt{2} \times 10^{-\frac{\mathrm{SINAD}}{20}} \ .$$

The DR corresponds to the way resolution is defined for metrological systems [40], that is, the resolution ρ in a metrological system is defined as

$$\rho = 6\sigma_t \ .$$

If the error $\tilde{y} - x$ can be approximated by a normally distributed noise realization, then $P(-3\sigma_t < \tilde{y} - x < 3\sigma_t) \approx 99.7\%$, and the range $6\sigma_t$ is a good approximation to the peak-to-peak value. For a DAC with range Δ, the DR is defined as:

$$\mathrm{DR} = \rho/\Delta \ .$$

Some of the power spectra used to produce the measurements in Tab. I are presented in Figs. 13, 14, 15, and 16.

TABLE I
MEASURED PERFORMANCE RESULTS.

Exp. No.	Filter Config.	Carrier Freq.	Carrier Amp.	HF Dither Amp.	SINAD	ENOB	DR	SNR	THD	Input Range
A	1)	99 Hz	100%	0%	93.4 dBc	15.2 bit	45.5 ppm	111 dB	-93.4 dBc	±10 V
B	1)	999 Hz	100%	0%	94.2 dBc	15.3 bit	41.6 ppm	111 dB	-94.2 dBc	±10 V
C	1)	99 Hz	50%	0%	89.1 dBc	14.5 bit	74.3 ppm	107 dB	-89.2 dBc	±5 V
D	1)	999 Hz	50%	0%	89.4 dBc	14.6 bit	72.2 ppm	107 dB	-89.4 dBc	±5 V
E	1)	99 Hz	50%	50%	104 dBc	17.0 bit	13.3 ppm	107 dB	-107 dBc	±5 V
F	1)	999 Hz	50%	50%	100 dBc	16.4 bit	20.4 ppm	106 dB	-102 dBc	±5 V
G	2)	99 Hz	50%	50%	102 dBc	16.7 bit	16.2 ppm	104 dB	-106 dBc	±5 V
H	2)	999 Hz	50%	50%	99.7 dBc	16.3 bit	22.1 ppm	104 dB	-102 dBc	±5 V
I	3)	99 Hz	100%	0%	94.7 dBc	15.4 bit	39.1 ppm	113 dB	-94.7 dBc	±10 V
J	3)	999 Hz	100%	0%	94.7 dBc	15.4 bit	39.1 ppm	113 dB	-94.8 dBc	±10 V
K	3)	99 Hz	50%	0%	90.7 dBc	14.8 bit	62.1 ppm	110 dB	-90.7 dBc	±5 V
L	3)	999 Hz	50%	0%	90.0 dBc	14.7 bit	66.9 ppm	110 dB	-90.1 dBc	±5 V
M	4)	99 Hz	50%	50%	105 dBc	17.2 bit	11.5 ppm	109 dB	-107 dBc	±5 V
N	4)	999 Hz	50%	50%	102 dBc	16.7 bit	16.5 ppm	108 dB	-103 dBc	±5 V

Filter Configurations (see Sec. VIII)
1) Notch filter (1 channel for carrier and HF dither)
2) Notch filter and differential amplifier (1 channel for carrier and HF dither and 1 channel for HF dither)
3) Notch filter and channel averaging (4 channels for carrier and HF dither)
4) Notch filter, differential amplifier, and channel averaging (4 channels for carrier and HF dither and 4 channels for HF dither)

TABLE II
RESULT COMPARISON FOR 99-HZ CARRIER SIGNALS.

Comp. No.	Exp. No.	Exp. No.	Change in Experimental Configuration	Metric	Expected Outcome	Difference in Result
(1)	A	C	a) Carrier amplitude reduced from 100% to 50%	SINAD	Decrease (worse)	-4.30 dB
				SNR	Decrease (worse)	-4.00 dB
				THD	Increase (worse)	4.20 dB
(2)	C	E	b) Application of HF dither	SINAD	Increase (better)	14.9 dB
				SNR	No change	0 dB
				THD	Decrease (better)	-17.8 dB
(3)	E	G	c) Subtraction of HF dither	SINAD	Decrease (worse)	-2.00 dB
				SNR	Decrease (worse)	-3.00 dB
				THD	No change	1.00 dB
(4)	C	K	d) Channel averaging	SINAD	Increase (better)	1.60 dB
				SNR	Increase (better)	3.00 dB
				THD	No change	-1.50 dB
(5)	I	M	a) Carrier amplitude reduced from 100% to 50% b) Application of HF dither	SINAD	Increase (better)	10.3 dB
				SNR	Decrease (worse)	-4.00 dB
				THD	Decrease (better)	-12.3 dB

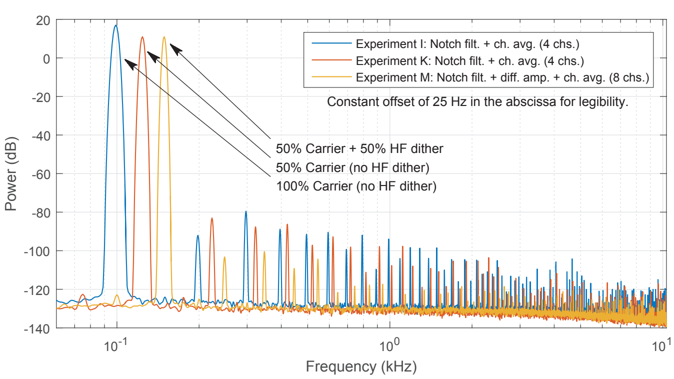

Fig. 14. **HF dither:** *Using filter configs. 3) and 4).* Spectra with a 99 Hz carrier signal that show the effect of the HF dither (reduced harmonic distortion) — 10.3 dB improvement.

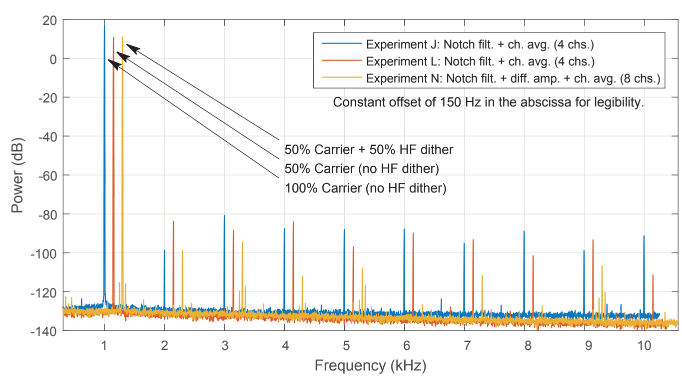

Fig. 15. **HF dither:** *Using filter configs. 3) and 4).* Spectra with a 999 Hz carrier signal that show the effect of the HF dither (reduced harmonic distortion) — 7.30 dB improvement.

X. DISCUSSION

Fig. 13 shows the effect of averaging DAC channels (Sec. V). The spectrum when using a single channel is compared to the spectrum when using four channels. It can

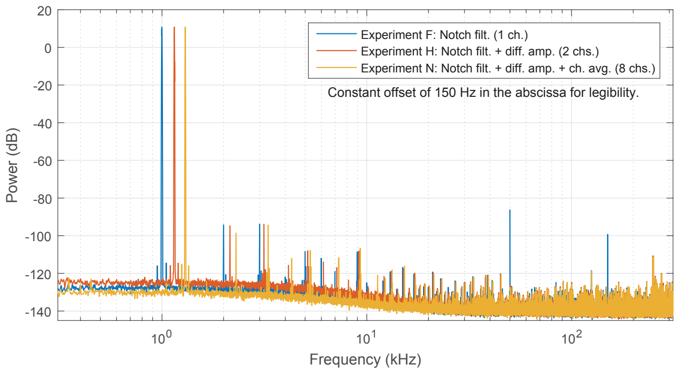

Fig. 16. **Differential amplifier and channel averaging:** *Using filter configs. 1), 2) and 4).* Spectra that show the effect of of the differential amplifier (improved removal of HF dither) and channel averaging (lower noise-floor).

be observed that the noise-floor is reduced, but the averaging has little effect on the harmonic distortion, see Tab. II(4).

The effect of the HF dither (Sec. IV-A) is illustrated in Fig. 14. The response from experiment I, using a 10-V carrier at 99 Hz, is compared to the response from experiment M, when using a 5-V carrier at 99 Hz and a 5-V HF dither at 50 kHz. It is apparent that the harmonic distortion is reduced. From the results comparison in Tab. II(5), the improvement in SINAD is 10.3 dB, even when the carrier amplitude has been reduced by 6.02 dB. Comparing the results for experiment C and E in Tab. II(2), where the same carrier amplitude has been used, an improvement in the SINAD of 14.9 dB can be seen. For these two experiments the THD differ by -17.8 dB. The performance gain is due to the reduction of harmonic distortion. Since the only change between the experiments is the addition of HF dither, the reduction in harmonic distortion is due to the smoothing effect the HF dither has on the INL. A similar comparison is presented in Fig. 15, with results from experiments J, L, and N, using a carrier at 999 Hz. The same effect is seen in this case, but the effect of the HF dither is reduced to a SINAD improvement of 7.30 dB.

At 99 Hz the carrier is well within the chosen baseband (10 kHz) and the decreased amplitude of the harmonics due to smoothing of the INL should be most noticeable. As the carrier frequency increases, some frequency components due to intermodulation will start to appear in the baseband, deteriorating performance. However, the spectrum will still be dominated by the harmonic distortion. As the carrier frequency increases towards the baseband cut-off, the higher-order harmonic components will move out of the baseband, and the performance will increase again. A carrier at 999 Hz results in approximately the worst-case performance.

Increasing the HF dither amplitude will further reduce the harmonic distortion. However, since the effective range is reduced, the contribution from the noise-floor starts to dominate and the SINAD decreases. Similarly, decreasing the HF dither amplitude increases the harmonic distortion, and the distortion becomes the dominant contribution among the unwanted output components; hence the SINAD will decrease. A dither amplitude of 50% was close to optimal for the experimental system used.

Fig. 16 shows the effect due to subtraction of the HF dither using the differential amplifier (Sec. VI) and channel averaging (Sec. V). The remaining fundamental frequency and first harmonic of the triangle-wave HF dither is observed to be removed by the differential amplifier, but at the expense of an increased noise-floor. By applying channel averaging, the noise-floor is reduced. The result comparison in Tab. II(3) confirms the worsening of the noise-floor when applying HF dither subtraction. Since the reduction of the remaining HF dither is outside of the baseband, it does not count towards a better SINAD.

There is a slightly higher noise-floor for the results recorded using an ADC input range of ± 10 V compared to the results when the input range is ± 5 V. The increase does introduce a small error in the SINAD and SNR measurements when using a ± 10 V range. As the harmonic distortion is the main contributor to the reduction of the SINAD, the noise-floor of the ± 10 V range measurements appears to be a negligible source of error. As a TPDF dither has been used for all the experiments, the non-linearity due to uniform quantization should be eliminated.

The presence of the HF dither will also reduce non-linearity in devices in the signal chain that is subjected to it. Hence, the notch filter will see some improvement when HF dither subtraction is not used, but the low-pass filter will not. The op-amps used in the summing stages in Fig. 11(c) will likely see an improvement, but the differential stage will not. The influence of the HF dither on the non-linearity of the ADC is also negligible.

XI. Conclusions

It was experimentally demonstrated that the dynamic performance of a digital-to-analog converter (DAC) can be improved by using a large high-frequency (HF) dither. The improvement is due to the smoothing effect the dither has on the non-linearity of the DAC. An improvement of the signal-to-noise-and-distortion ratio (SINAD) of more than 10 dB was achieved. It is straight-forward to retrofit the method to an existing, sufficiently fast DAC, as it only requires generation of the HF dither and a suitable analog filter for attenuation of the dither in the output. Further improvements in SINAD can be achieved by subtracting the dither using two channels and a differential amplifier, and by reducing the noise-floor using averaging of several channels.

Acknowledgments

This work was supported in part by the Australian Research Council Discovery Project DP120100487 and the Future Fellowship FT130100543.

References

[1] I. Galton and P. Carbone, “Rigorous error analysis of D/A conversion with dynamic element matching,” *IEEE Trans. Circuits Syst. II, Analog Digit. Signal Process.*, vol. 42, no. 12, pp. 763–772, 1995.
[2] I. Galton, “Why Dynamic-Element-Matching DACs Work,” *IEEE Trans. Circuits Syst. II*, vol. 57, no. 2, pp. 69–74, 2010.
[3] R. J. Van De Plassche, “Dynamic Element Matching for High-Accuracy Monolithic D/A Converters,” *IEEE J. Solid-State Circuits*, vol. 11, no. 6, pp. 795–800, 1976.

[4] R. Schreier and G. C. Temes, *Understanding Delta-Sigma Data Converters*. IEEE Press, 2005.

[5] M. Frey and H.-A. Loeliger, "On the Static Resolution of Digitally Corrected Analog-to-Digital and Digital-to-Analog Converters With Low-Precision Components," *IEEE Trans. Circuits Syst. I*, vol. 54, no. 1, pp. 229–237, 2007.

[6] M. J. Pelgrom, *Analog-to-Digital Conversion*, 2nd ed. Springer-Verlag, 2013.

[7] T. Cataltepe, A. R. Kramer, L. E. Larson, G. C. Temes, and R. H. Walden, "Digitally corrected multi-bit $\Sigma\Delta$ data converters," *Circuits and Systems, 1989., IEEE International Symposium on*, pp. 647–650, 1989.

[8] J. Arias, P. Kiss, V. Boccuzzi, L. Quintanilla, L. Enriquez, J. Vicente, D. Bisbal, J. S. Pablo, and J. Barbolla, "Nonlinearity Correction for Multibit Delta-Sigma DACs," *IEEE Trans. Circuits Syst. I*, vol. 52, no. 6, pp. 1033–1041, 2005.

[9] D. W. J. Groeneveld, H. J. Schouwenaars, H. A. H. Termeer, and C. A. A. Bastiaansen, "A Self-calibration Technique for Monolithic High-resolution D/A Converters," *IEEE J. Solid-State Circuits*, vol. 24, no. 6, pp. 1517–1522, 1989.

[10] L. Risbo, R. Hezar, B. Kelleci, H. Kiper, and M. Fares, "Digital Approaches to ISI-Mitigation in High-Resolution Oversampled Multi-Level D/A Converters," *IEEE Journal of Solid-State Circuits*, vol. 46, no. 12, p. 2892, 2011.

[11] K. Wakabayashi, K. Kato, T. Yamada, O. Kobayashi, H. Kobayashi, F. Abe, and K. Niitsu, "Low-Distortion Sinewave Generation Method Using Arbitrary Waveform Generator," *J Electron Test*, vol. 28, no. 5, pp. 641–651, 2012.

[12] F. Abe, Y. Kobayashi, K. Sawada, K. Kato, O. Kobayashi, and H. Kobayashi, "Low-Distortion Signal Generation for ADC Testing," in *IEEE International Test Conference*. IEEE, 2014, pp. 1–10.

[13] B. K. Vasan, S. K. Sudani, D. J. Chen, and R. L. Geiger, "Low-Distortion Sine Wave Generation Using a Novel Harmonic Cancellation Technique," *IEEE Trans. Circuits Syst. I*, vol. 60, no. 5, pp. 1122–1134, 2013.

[14] M. J. Barragan, G. Leger, D. Vazquez, and A. Rueda, "On-chip sinusoidal signal generation with harmonic cancelation for analog and mixed-signal BIST applications," *Analog Integr Circ Sig Process*, vol. 82, no. 1, pp. 67–79, 2014.

[15] C. Shi and E. Sanchez-Sinencio, "150—850 MHz High-Linearity Sine-wave Synthesizer Architecture Based on FIR Filter Approach and SFDR Optimization," *IEEE Trans. Circuits Syst. I*, vol. 62, no. 9, pp. 2227–2237, 2015.

[16] Y. K. Yong, S. O. R. Moheimani, B. J. Kenton, and K. K. Leang, "Invited Review Article: High-speed flexure-guided nanopositioning: Mechanical design and control issues," *Rev. Sci. Instrum.*, vol. 83, no. 12, p. 121101 (22 pages), 2012.

[17] R. Oldenburger and R. C. Boyer, "Effects of Extra Sinusoidal Inputs to Nonlinear Systems," *J Basic Eng-T ASME*, vol. 84, no. 4, pp. 559–569, 1962.

[18] G. Zames and N. A. Shneydor, "Dither in Nonlinear Systems," *IEEE Trans. Autom. Control*, vol. 21, no. 5, pp. 660–667, 1976.

[19] S. Mossaheb, "Application of a method of averaging to the study of dithers in non-linear systems," *Int J Control*, vol. 38, no. 3, pp. 557–576, 1983.

[20] L. Iannelli, K. H. Johansson, U. T. Jönsson, and F. Vasca, "Averaging of nonsmooth systems using dither," *Automatica*, vol. 42, no. 4, pp. 669–676, 2006.

[21] L. Schuchman, "Dither Signals and Their Effect on Quantization Noise," *IEEE Trans. Commun. Technol.*, vol. 12, no. 4, pp. 162–165, 1964.

[22] A. B. Sripad and D. Snyder, "A necessary and sufficient condition for quantization errors to be uniform and white," *IEEE Trans. Acoust., Speech, Signal Process.*, vol. 25, no. 5, pp. 442–448, 1977.

[23] B. Widrow, I. Kollar, and M.-C. Liu, "Statistical Theory of Quantization," *IEEE Trans. Instrum. Meas.*, vol. 45, no. 2, pp. 353–361, 1996.

[24] R. M. Gray and D. L. Neuhoff, "Quantization," *IEEE Trans. Inf. Theory*, vol. 44, no. 6, pp. 2325–2383, 1998.

[25] R. A. Wannamaker, S. Lipshitz, J. Vanderkooy, and J. N. Wright, "A Theory of Nonsubtractive Dither," *IEEE Trans. Signal Process.*, vol. 48, no. 2, pp. 499–516, 2000.

[26] B. Widrow and I. Kollár, *Quantization Noise*. Cambridge University Press, 2008.

[27] N. A. Pendergrass and J. S. Farnbach, "A high-resolution, low-frequency spectrum analyzer," *Hewlett-Packard Journal*, 1978.

[28] R. A. Belcher, "The use of multi tone dither in high speed A/D conversion," in *Advanced A-D and D-A Conversion Techniques and their Applications, Second Intl. Conf. on*. IEE, 1994, pp. 153–158.

[29] P. Carbone and D. Petri, "Effect of Additive Dither on the Resolution of Ideal Quantizers," *IEEE Trans. Instrum. Meas.*, vol. 43, no. 3, pp. 389–396, 1994.

[30] M. J. Flanagan and G. A. Zimmerman, "Spur-reduced digital sinusoid synthesis," *IEEE Trans. Commun.*, vol. 43, no. 7, pp. 2254–2262, 1995.

[31] J. Vanderkooy and S. P. Lipshitz, "Resolution Below the Least Significant Bit in Digital Systems with Dither," *J. Audio Eng. Soc.*, vol. 32, no. 3, pp. 106–113, 1984.

[32] M. F. Wagdy and M. Goff, "Linearizing Average Transfer Characteristics of Ideal ADC's via Analog and Digital Dither," *IEEE Trans. Instrum. Meas.*, vol. 43, no. 2, pp. 146–150, 1994.

[33] I. De Lotto and G. E. Paglia, "Dithering improves A/D converter linearity," *IEEE Trans. Instrum. Meas.*, vol. IM-35, no. 2, pp. 170–177, 1986.

[34] B. A. Blesser and B. N. Locanthi, "The Application of Narrow-Band Dither Operating at the Nyquist Frequency in Digital Systems to Provide Improved Signal-to-Noise Ratio over Conventional Dithering," *J. Audio Eng. Soc.*, vol. 35, no. 6, pp. 446–454, 1987.

[35] M. Bartz, "Large-scale dithering enhances ADC dynamic range," *Microwaves & RF*, vol. 32, no. 5, pp. 192–194, 196, 198, 1993.

[36] P. Carbone, C. Narduzzi, and D. Petri, "Dither Signal Effects on the Resolution of Nonlinear Quantizers," *IEEE Trans. Instrum. Meas.*, vol. 43, no. 2, pp. 139–145, 1994.

[37] M. F. Wagdy, "Effect of Additive Dither on the Resolution of ADC's with Single-Bit or Multibit Errors," *IEEE Trans. Instrum. Meas.*, vol. 45, no. 2, pp. 610–615, 1996.

[38] S. A. Leyonhjelm, M. Faulkner, and P. Nilsson, "An Efficient Implementation of Bandlimited Dithering," *Wireless Pers Commun*, vol. 8, no. 1, pp. 31–36, 1998.

[39] H. Czichos, T. Saito, and L. Smith, Eds., *Springer Handbook of Metrology and Testing*, 2nd ed. Springer-Verlag, 2008.

[40] A. J. Fleming and K. K. Leang, *Design, Modeling, and Control of Nanopositioning Systems*. Springer-Verlag, 2014.

[41] W. B. Cleveland, "First-Order-Hold Interpolation Digital-to-Analog Converter with Application to Aircraft Simulation," NASA, Tech. Rep., 1976.

[42] R. E. Crochiere and L. Rabiner, "Interpolation and decimation of digital signals—A tutorial review," in *Proc. IEEE*. IEEE, 1981, pp. 300–331.

[43] S. P. Lipshitz, R. A. Wannamaker, and J. Vanderkooy, "Quantization and Dither: A Theoretical Survey," *J. Audio Eng. Soc.*, vol. 40, no. 5, pp. 355–375, 1992.

[44] R. H. Walden, "Analog-to-Digital Converter Survey and Analysis," *IEEE J. Sel. Areas Commun.*, vol. 17, no. 4, pp. 539–550, 1999.

[45] J. A. Connelly and K. P. Taylor, "An Analysis Methodology to Identify Dominant Noise Sources in D/A and A/D Converters," *IEEE Trans. Circuits Syst.*, vol. 38, no. 10, pp. 1133–1144, 1991.

[46] P. Horowitz and W. Hill, *The Art of Electronics*, 3rd ed. Cambridge University Press, 2015.

[47] J. J. Bussgang, L. Ehrman, and J. W. Graham, "Analysis of nonlinear systems with multiple inputs," *Proc. IEEE*, vol. 62, no. 8, pp. 1088–1119, 1974.

[48] E. Balestrieri and S. Rapuano, "Defining DAC performance in the frequency domain," *Measurement*, vol. 40, no. 5, pp. 463–472, 2007.

[49] D. Rijlaarsdam, P. Nuij, J. Schoukens, and M. Steinbuch, "Spectral analysis of block structured nonlinear systems and higher order sinusoidal input describing functions," *Automatica*, vol. 47, no. 12, pp. 2684–2688, 2011.

[50] K. A. Simons, "The decibel relationships between amplifier distortion products," in *Proc. IEEE*. IEEE, 1970, pp. 1071–1086.

[51] X. Wu, Z. Q. Lang, and S. A. Billings, "Analysis of Output Frequencies of Nonlinear Systems," *IEEE Trans. Signal Process.*, vol. 55, no. 7, pp. 3239–3246, 2007.

[52] W. R. Bennett, "Spectra of Quantized Signals," *Bell System Technical Journal*, vol. 27, no. 3, pp. 446–472, 1948.

[53] N. M. Blachman, "The intermodulation and distortion due to quantization of sinusoids," *IEEE Trans. Acoust., Speech, Signal Process.*, vol. 33, no. 6, pp. 1417–1426, 1985.

[54] L. Ljung, *System Identification: Theory for the User*, 2nd ed. Prentice Hall, Inc., 1999.

[55] D. P. Bertsekas and J. N. Tsitsiklis, *Introduction to Probability*, 2nd ed. Athena Scientific, 2008.

[56] E. M. Stein and R. Shakarchi, *Real Analysis*. Princeton University Press, 2005.

[57] T. Tao, *An Introduction to Measure Theory*. American Mathematical Society, 2011.

[58] J. F. Kaiser and R. W. Schafer, "On the Use of the I_0-Sinh Window for Spectrum Analysis," *IEEE Trans. Acoust., Speech, Signal Process.*, vol. 28, no. 1, pp. 105–107, 1980.

[59] J. R. Bainter, "Active filter has stable notch, and response can be regulated," *Electronics*, vol. 48, pp. 115–117, 1975.

[60] R. H. S. Riordan, "Simulated Inductors Using Differential Amplifiers," *IEE Electron. Lett.*, vol. 3, no. 2, pp. 50–51, 1967.

[61] H. Hall, "RC Networks with Single-Component Frequency Control," *IRE T. Circuit Theory*, vol. 2, no. 3, pp. 283–284, 1955.

[62] R. P. Sallen and E. L. Key, "A practical method of designing RC active filters," *IRE T. Circuit Theory*, vol. 2, no. 1, pp. 74–85, 1955.

Arnfinn A. Eielsen received the Siv.Ing. (MSc) degree and the Ph.D. degree in Engineering Cybernetics from the Norwegian University of Science and Technology, Trondheim, Norway in 2007 and 2012, respectively. He is currently employed as a research fellow in the School of Electrical Engineering and Computer Science at the University of Newcastle, Australia. Research interest include mathematical modeling, identification, adaptive systems, motion control, and control theory in general. He is a member of IEEE.

Andrew J. Fleming graduated from the University of Newcastle, Australia with a Bachelor of Electrical Engineering in 2000 and Ph.D. in 2004. He is presently an Australian Research Fellow and Senior Lecturer at the School of Electrical Engineering and Computer Science, The University of Newcastle, Australia. His research includes nanopositioning, high-speed scanning probe microscopy, microcantilever sensors, metrological position sensors, and optical nanofabrication. Academic awards include the University of Newcastle Vice-Chancellors Award for Researcher of the Year and the IEEE Control Systems Society Outstanding Paper Award for research published in the IEEE Transactions on Control Systems Technology. Dr. Fleming is the co-author of three books, several patent applications and more than 100 Journal and Conference papers.